

COMMISSIONING OF THE LNLS X-RAY BPMS

S. Marques[#], P. F. Tavares LNLS, Campinas, Brazil

Abstract

We present experimental results of the commissioning of staggered-pair blade X-Ray beam position monitor (XBPM) recently developed and installed at the diagnostic beamline of the UVX electron storage ring at the Brazilian Synchrotron Light Laboratory (LNLS). The results obtained with a prototype XBPM indicate that the short-term and long-term data are both in agreement with the data from a commercially acquired XBPM installed at the same beamline, as well as with the data of the electron storage ring RF BPMs. In this paper we present the commissioning results of the LNLS XBPM.

INTRODUCTION

The tests with the first XBPM installed at the LNLS diagnostic beamline started in the beginning of 2005 [1]. Since that time, no modification has been made to the body of the XBPM that is composed basically of two staggered copper blade pairs positioned to intercept only the edges of the vertical distribution of the X-Ray (XR) beam.

XBPM GAIN, LINEARITY AND RESOLUTION OPTIMIZATION

Figure 1 shows the blades positioning scheme and the main parameters of the XBPM geometry. The beam position can be determined according the equation 1.

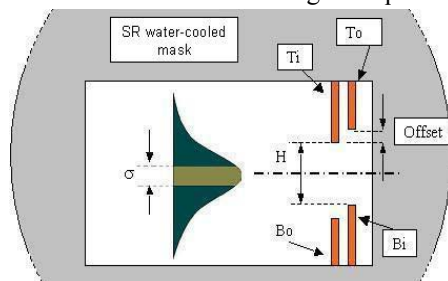


Figure 1: XBPM blades disposition. The blades are named: Top inside (Ti), Top outside (To), Bottom inside (Bi) and Bottom outside (Bo). The offset used in both commercial and LNLS XBPM is 1 mm. H is the separation between the two pairs and it is 7 mm for both XBPMs. The XBPMs are installed 8.5 m from the source and the vertical RMS size σ is about 3.26 mm at this point. All the blades are 2 mm thickness and are electrically isolated by 0.5 mm alumina plates. The 20 mm x 74 mm aperture in the refrigerated synchrotron radiation mask limits the illuminated area of the blades.

$$Position = -\left(\frac{\Delta S_{Ti,Bo}}{\Delta S_{To,Bi} - \Delta S_{Ti,Bo}}\right) - \frac{Offset}{2} \quad (1)$$

In Eq. 1, ΔS denotes the difference divided by the sum of the photocurrents of each blade pair. It is possible to calculate the relationship between the photocurrents through the beam parameters (vertical distribution and centroid position) and through the geometry of the blades (active length, H and offset). For a fixed XBPM geometry, the position depends basically on the intensities of the photocurrents and the beam vertical distribution, so it is possible to evaluate the XBPM theoretical performance by the equation 1.

XBPM Gain and Linearity Analysis

The relationship between the calculated beam position and the beam centroid displacements, in other words, the gain, can be obtained by differentiating equation 1. The results show that there are optimum values of offset and distance H for reaching good linearity in a ± 0.5 mm range for a given vertical beam size. Figure 2 shows the effect of four XBPM geometries over the XBPM gain and linearity.

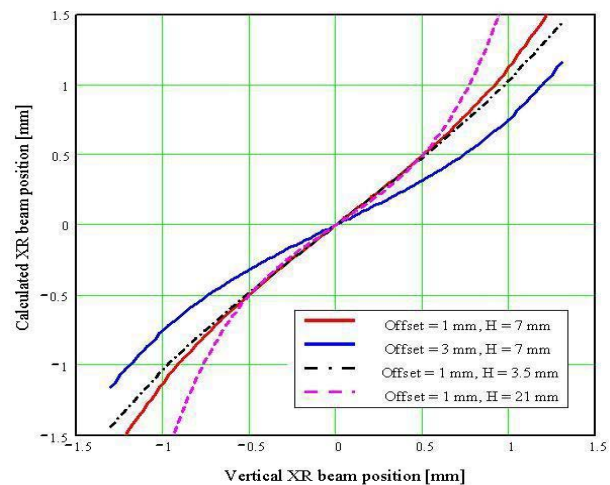


Figure 2: XBPM behaviour for different offsets and blades' separation distances. The beam size, source to monitor distance and blades active area were fixed in their real values.

Figure 2 shows that decreasing the distance H makes the XBPM linear in a bigger range, but the amplified blade currents increase the requirements of the water-cooled mask. The gain and linearity are negatively affected by increasing the offset distance. Decreasing the offset distance below 1 mm does not change these two parameters.

XBPM Resolution Analysis

Assuming that the main uncertainty source in the position measurement is the electrical noise in the converted photocurrents' signals, the resolution of the XBPM can be evaluated by an error propagation analysis

[#]sergio@lnls.br

of Eq. 1. Figure 3 shows the RMS resolution of the XBPM for different geometries.

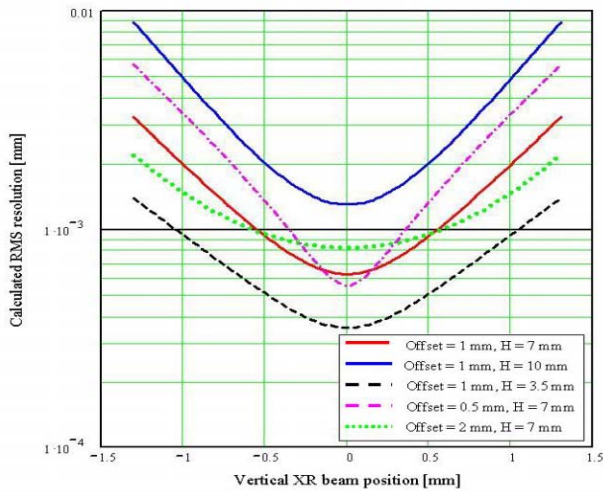


Figure 3: XBPM RMS resolution dependence on different offsets and H values. The beam size, source to monitor distance and blades active area were fixed in their real values. The noise level of the LNLS XBPM electronics (after filtering) is 5 nA RMS, which corresponds to 0.05% of the average blade currents in a typical shift.

Figure 3 shows that for any XBPM geometry, the resolution is better when the XR beam is centred. Increasing the offset distance above 1 mm decreases the XBPM resolution in the linear range. Decreasing the offset below 1 mm improves the resolution only in a small portion of the linear region. The smaller the H, the higher the resolution.

XBPM CHARACTERIZATION

Through the considerations above, it is possible to see that the gain, resolution and linearity of the position measurements are very dependent of the XBPM geometry and the vertical beam size. Experiments were performed to determine the dependence of the XBPM gain, resolution and linearity on the XR vertical beam size, position and intensity.

There are two XBPMs (monitor and electronics) installed at the LNLS diagnostic beamline, one commercial, acquired from FMB and another completely developed at the LNLS. The commercial XBPM was installed in a high precision Z translation stage, which allows vertical movements of the XBPM in steps smaller than 1 μm . The homemade XBPM is fixed in the vacuum chamber flanges and cannot be moved in the vertical plane.

Not all the experiments were done with both XBPMs simultaneously (using electron beam movements). For non-linearity observation for example, the vertical correctors did not allow us to make parallel movements of the beam in a wide enough range. In all the experiments we took advantage of the small distance between the two monitors (355 mm) for comparing the results. The next topics describe some results of the characterization experiments.

In all experiments the blades were biased with -100 V to avoid crosstalk among them and space charge effects.

LNLS XBPM Gain with Respect to Commercial XBPM Gain

At the beginning of the experiments, we confirmed that the two XBPMs installed at the diagnostic beamline had identical behaviour in the linear region by using parallel movements of the beam to characterize both XBPMs. Figure 4 shows the relationship between the two XBPMs for parallel beam movements.

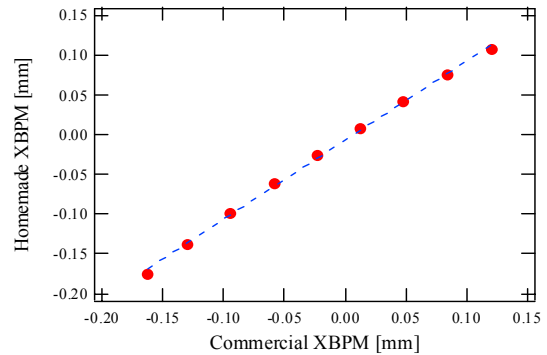


Figure 4: Relationship of the two XBPMs. Gain = 0.992 ± 0.0147 , Offset = -0.0069 ± 0.0014 . Coefficient values \pm one standard deviation.

LNLS and Commercial XBPM Gains with Respect to Electron Beam RF BPMs

Figure 4 shows the XBPMs are identical in the linear region, but in the same experiment, which used parallel movements of the beam, both XBPMs showed gains of about 1.3 with respect to electron beam RF BPMs. These gains are affected by the XBPM geometry, by differences among the blades material and by the differences between the assumed and the real vertical beam size at the point of the position measurement. It seems that small construction errors or small blades positioning errors could better explain this 30% difference, but we do not determine which factor contributes more for this gain error or why the gain errors of the XBPMs are similar.

However the characterization showed that the gains are not affected either by the beam intensity or by changes in the vertical electron beam size. Figure 5 shows the relationship between the homemade XBPM gain and beam intensity. Figure 6 shows the relationship between the commercial XBPM gain and the beam intensity.

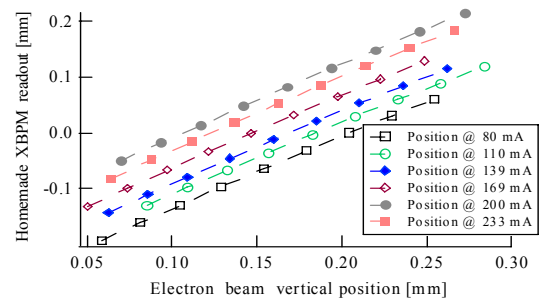


Figure 5: Homemade XBPM positions Vs electron beam positions for different intensities. The average gain is $1.30 \pm 2.4\%$ (peak-to-peak).

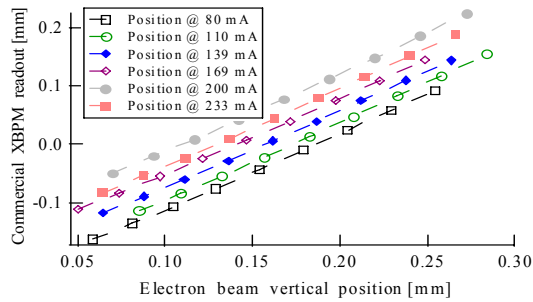


Figure 6: Commercial XBPM positions Vs electron beam positions for different intensities. The average gain is 1.33 and the $\pm 2.6\%$ (peak-to-peak).

In the figures 5 and 6, the gain fluctuation observed among the curves is probably due to orbit drifts during each experiment. Also in these two figures, arbitrary offsets were included in the curves to separate them.

XBPM Gain Vs Electron Beam Size

There is an XR pinhole camera installed at the same beamline of the XBPMs that allows electron beam size measurements with μm resolution. In the normal mode of operation, the RMS vertical beam size measured in the dipole of the diagnostic beamline is $90\ \mu\text{m}$, and decreases less than 5% during the shift.

Changing the coupling factor of the electron beam through the skew quadrupoles, we increased the RMS vertical beam size from $77\ \mu\text{m}$ up to $121\ \mu\text{m}$ and any noticeable change in the XBPMs gain was observed. Figure 7 shows the commercial XBPM gain versus the RMS vertical beam size.

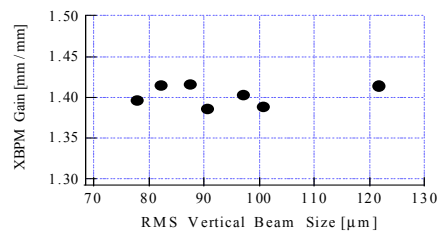


Figure 7: XBPM gain Vs RMS vertical electron beam size. The $\pm 1.1\%$ peak-to-peak gain fluctuation observed probably is due orbit corrections during the experiments.

The measurement showed by figure 7 was performed moving the translation stage of the commercial XBPM. The 5% gain difference between the experiments described by figures 6 and 7 can be attributed to gain and offset errors in the RF BPMs, since the Z table was carefully calibrated. The LNLS XBPM gain showed the same behaviour regarding the beam size variations.

XBPM Resolution

At the beginning of the tests in early 2005, we attributed the peak-to-peak “noise” observed in the XBPMs signals during few minutes to the electrical noise present in the blade signals, but a closer observation of the position information delivered by the XBPMs shows that it is strongly correlated with the electron beam motion. During an accelerator physics shift without orbit feedback, we noticed that we could predict the XBPM behaviour to within $2.5\ \mu\text{m}$ by means of a linear

transformation of the data from the two RF BPMs located around the dipole magnet which serves as the source of the XR beam the XBPM. The remaining error was smoothly distributed in the whole shift. In order to calculate the XBPM data from the RF BPMs data, we considered the distance between the RF BPMs, the distance between the XBPM and the beamline dipole and a correction factor (gain) was applied in the XBPM data. Figure 8 shows the positions given by the two RF BPMs before and after the diagnostic beamline dipole, the position given by the LNLS XBPM and the error between the calculated and real XBPM data.

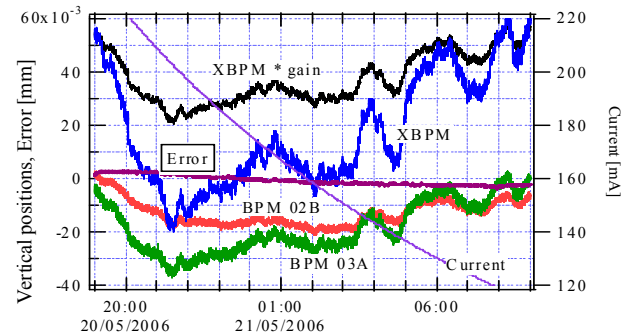


Figure 8: The positions given by the two RF BPMs around the diagnostic beamline dipole, the position given by the LNLS XBPM and the error between the calculated and real XBPM data.

CONCLUSION

The characterization of both XBPMs confirmed our expectation that X-Ray position can be very useful for electron beam stability monitoring purposes. We hope the future experiments including the LNLS XBPM in the feedback loop validates our plan of installing XBPMs in the beamline front-ends to improve even more the beam stability for the users.

The characterization showed us that translating the XBPM body is extremely important for the commissioning period. Since there will be small differences among the various XBPMs to be installed in the LNLS beamlines, the mechanical design will be modified to allow at least few mm of vertical translation.

The simulations [2] performed with the XBPM parameters allowed us to better understand its highly non-linear behaviour. Besides that, the calculated resolution and non-linearity parameters corroborated with the measured parameters. The 30% gain difference of the XBPMs with respect to the RF BPMs is under investigation.

REFERENCES

- [1] S. R. Marques, et. al., “An X-RAY BPM and Accompanying Electronics”, PAC’05, Knoxville, May 2005, p. 3019.
- [2] P. F. Tavares, S. R. Marques, “LNLS XBPMs design and optimization”, LNLS memorandum. To be published.